

Microstructural Development of Adiabatic Shear Bands Formed by Ballistic Impact in a WELDALITE 049 Alloy

CHANG GIL LEE, WOO JIN PARK, SUNGHAK LEE, and KWANG SEON SHIN

The object of the present study is to investigate the microstructural development of the adiabatic shear band formed by ballistic impact in a WELDALITE 049 alloy. The microstructure of the shear band was examined by optical microscopy and transmission electron microscopy. The results indicated that the adiabatic shear band consisted of fine recrystallized grains with a high dislocation density. This microstructure was considered to be formed in an extremely short time by the combined effects of the highly localized shear deformation and the high-temperature rise that occurred within the shear band. However, no precipitates could be observed in the interior of the grains, since the temperature rise in the shear band formation process was inferred to be above 460 °C and below the solidus temperature. Dynamic recrystallization was suggested as a possible mechanism to explain the microstructural development of the adiabatic shear band formed in the WELDALITE alloy.

I. INTRODUCTION

ONE of the characteristics arising from high-strain-rate loading is the formation of adiabatic shear bands caused by highly localized plastic deformation.^[1-9] In the process of adiabatic shear band formation, the temperature of the localized region rises radically due to the lack of time for the heat generated by the deformation to be emitted to the exterior.^[10-13] Such a radical local temperature rise has a softening effect on materials, accelerating plastic instability^[13,14] as well as inducing microstructural modifications such as phase transformation and recrystallization.^[9,15,16] This also reduces the load-carrying capacity within adiabatic shear bands, causing final failure of the structures.^[10-12,15] Thus, many studies on adiabatic shear band formation have actively been conducted in the areas of the defense and processing industries. However, there are still many uncertainties, especially regarding the microstructural development within the adiabatic shear band and the mechanism of its formation.

Wittman *et al.*^[14] investigated the microstructure after the ballistic impact test of an AISI 4340 steel and reported on the formation of a martensitic structure containing χ carbides due to the heat that is generated from the localized deformation at the time of the adiabatic shear band formation. Wingrove^[15] examined adiabatic shear bands of a tempered 1.0 pct C-1.0 pct Cr steel, and presented an article which showed the microstructure to have a high dislocation density and cell structure; in this article, he acknowledged the possibility of phase transformation. Recently, Cho *et al.*^[13] investigated the microstructure of adiabatic shear bands formed during the dynamic torsional testing of an

HY-100 steel and explained the mechanism of the microstructural development within the shear bands in terms of the dynamic recovery process. There have been many other studies conducted on adiabatic shear bands, but each study has had a different approach and theoretical background, in terms of dynamic recovery,^[7,13,14,16] dynamic recrystallization,^[17,18,19] and phase transformation.^[2,14,20] Thus, more studies should be conducted to clarify the formation mechanism and any factors involved in it. Especially, there have been few studies done on the mechanisms of adiabatic shear band formation and the microstructural development of aluminum alloys widely used for structural materials. In the present study, ballistic impact tests were conducted on a WELDALITE* 049 alloy, which has recently attracted much

*WELDALITE is a trademark of Lockheed Martin, Baltimore, MD.

interest as a lightweight armor material, and the microstructural development during adiabatic shear band formation was examined in detail by a transmission electron microscope (TEM).

II. EXPERIMENTAL

In this study, the ballistic impact tests were conducted on a WELDALITE 049 alloy, which has been developed by the Reynolds Metals Company (Richmond, VA) to improve weldability with the composition base of Al-Cu-Mg-Li-Ag. The target specimen of the WELDALITE alloy was sized to 100 × 100 × 12.8 mm. The flying speed of the projectile was about 830 m/s, and the flying direction was normal to the rolling direction of the target plate, as shown in Figure 1. Tables I and II contain the chemical composition and room-temperature tensile properties of the WELDALITE 049 alloy, respectively. Its microstructure has quite elongated grains in the rolling direction (Figure 2).

After the ballistic impact test, the target specimens were collected to investigate the microstructure of the adiabatic shear bands. The microhardness was measured under a 25-g load using a microvickers hardness tester in 20- μ m intervals from the center of the shear band. The perforated region of the specimen was sectioned parallel to the rolling

CHANG GIL LEE, Senior Researcher, is with the Materials Engineering Department, Korea Institute of Machinery and Materials, Changwon, 641-010 Korea. WOO JIN PARK, Research Scientist, is with the Advanced Materials Division, Research Institute of Industrial Science and Technology, Pohang, 790-600 Korea. SUNGHAK LEE, Professor, is with the Center for Advanced Aerospace Materials, Pohang University of Science and Technology, Pohang, 790-784 Korea. KWANG SEON SHIN, Associate Professor, is with the School of Materials Science and Engineering, Seoul National University, Seoul, 151-742 Korea.

Manuscript submitted March 31, 1997.

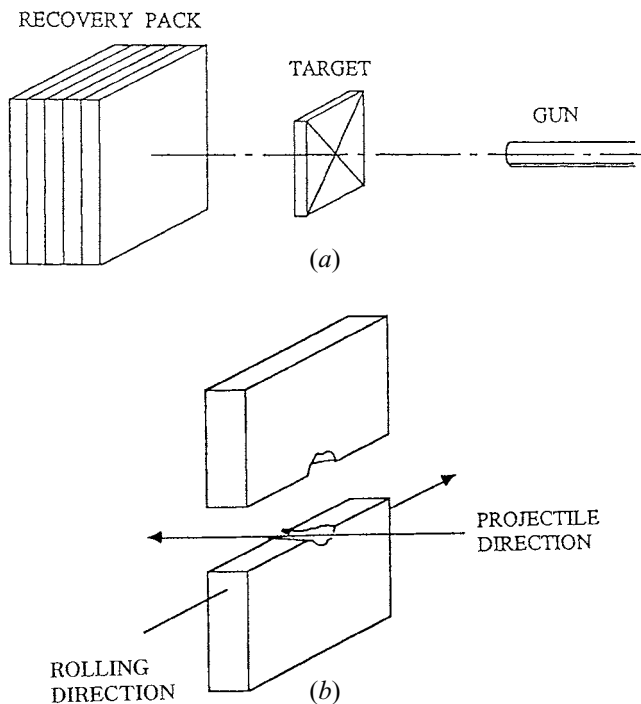


Fig. 1—Schematic diagrams of (a) the ballistic impact test system and (b) the projectile direction and the rolling direction in the test specimen.

Table I. Chemical Composition of a WELDALITE 049 Alloy (Weight Percent)

Cu	Li	Mg	Zr	Ag	Al
5.4	1.3	0.4	0.14	0.4	bal

direction, polished, etched, and observed by an optical microscope. In addition, TEM observation was carried out to examine the detailed microstructure of the adiabatic shear bands. First, the region including the adiabatic shear band was precisely sectioned and polished to prepare a thin specimen with a thickness of about 100 μm . After the shear band was made visible by light etching and the position was marked, a disc with 3-mm diameter was prepared, with the shear band being centralized. The disc specimen was further thinned by dimpling to a minimum thickness of 40 to 50 μm centered on the shear band. Final electropolishing was carried out in nital solution. Thin foils were examined using a TEM (PHILIPS* CM30) operated at 300 kV.

*PHILIPS is a trademark of Philips Electronic Instruments Corp., Mahwah, NJ.

III. RESULTS

A. Characteristics of Adiabatic Shear Band

Figure 3 is a micrograph of the WELDALITE alloy, and shows an adiabatic shear band. The width of the shear band is 15 to 20 μm , and a crack is propagated along the band. The shear strain within the band is about 1500 pct. The adiabatic shear band can generally be divided into the deformed shear band and the transformed shear band, depending on the band shape.^[8,14] The shear band in Figure 3 lacks continuity between the shear band and the surround-

Table II. Room-Temperature Tensile Properties of the WELDALITE 049 Alloy

Yield Strength (MPa)	Tensile Strength (MPa)	Tensile Elongation (Pct)
630	646	9

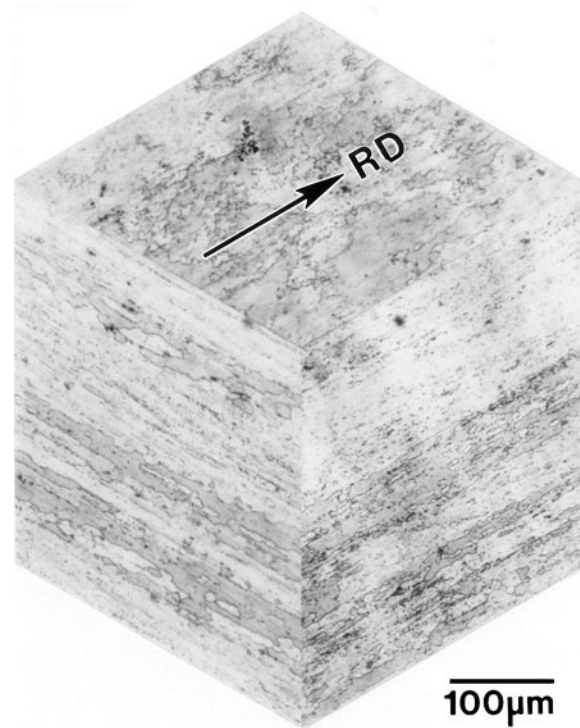


Fig. 2—Three-dimensional optical micrograph of the WELDALITE alloy used.

ing grains, and the interior microstructure of the transformed shear band is shaped differently than the surrounding matrix. This is known to occur as a result of the internal microstructural modification upon the shear band formation, arising from the localization of shear deformation and the effect of the temperature rise.^[14]

Figure 4 shows the microvickers hardness data. Within the band, the hardnesses are quite high compared to the surrounding matrix. It was reported that the hardness values around the adiabatic shear band of the HY-100 steel were lower than those in the matrix regions farther away from the shear band.^[13,21] This is associated with heat-affected zones formed by the sudden temperature rise. However, in the WELDALITE alloy, it is not likely that a heat-affected zone is formed around the shear band, judging from the alloy's tendency to vary in hardness.

B. TEM Observation

Figures 5(a) through (c) are dark-field TEM images and selected area diffraction patterns of major precipitates, *i.e.*, the S' -(Al_2CuMg), T_1 -(Al_2CuLi), and θ' -(Al_2Cu) phases, respectively. Because the WELDALITE alloy has a lithium content about half that of the 2090 or 8090 Al-Li alloys and the δ' -(Al_3Li) phases are mostly dissolved during precipitation and growth of the T_1 phases,^[22,23,24] they are not

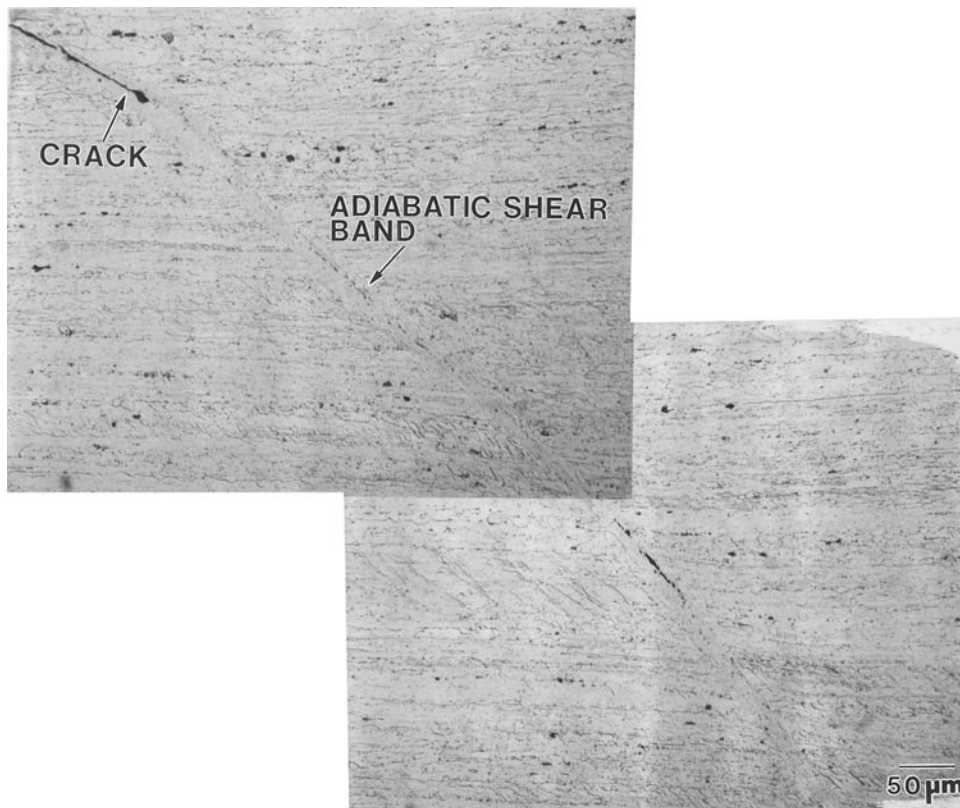


Fig. 3—Optical micrograph of the ballistically impacted specimen, showing an adiabatic shear band and a crack.

well observed in the WELDALITE alloy. The WELDALITE alloy also contains a small amount of Ag, as shown in Table I, which precipitates as Ω phases containing Ag and Mg and gives the additional precipitation hardening effect.^[25,26] It is reported that the Ω phases have a habit plane of $\{111\}$ and a similar structure to the T_1 phases.^[26] However, their existence within the WELDALITE alloy, the hardening mechanism of the Ag addition, and their effect on mechanical properties have not been clarified yet.

Figure 6 is a montage of bright-field TEM images showing the adiabatic shear band in its entire width. There seems to be no microstructural development in the boundary region between the shear band and the matrix. However, the interior of the shear band is composed of fine, equiaxed grains, which get finer as they reach the center. The grain size in the band center is below $0.4 \mu\text{m}$, as shown in Figures 7(a) and (b). The selected area diffraction pattern of this region shows a ring pattern, as shown in Figure 7(c), indicating an unorderly alignment of grains due to the large orientation difference between grains. An analysis of this orientation difference by a microdiffraction pattern at the $\langle 111 \rangle$ zone axis reveals that the cases of an orientation difference of less than 10 deg account for less than 3 pct of the total, while 90 pct of the cases show an orientation difference of over 20 deg .

Figure 8 is a higher-magnification TEM micrograph showing grains formed within the shear band. Dislocations with a very high density can be observed in many of these grains, indicating that they were under heavy deformation in the band formation. Using a tilting technique, most grains are confirmed to have a high dislocation density. However, a few grains show a low dislocation density, in

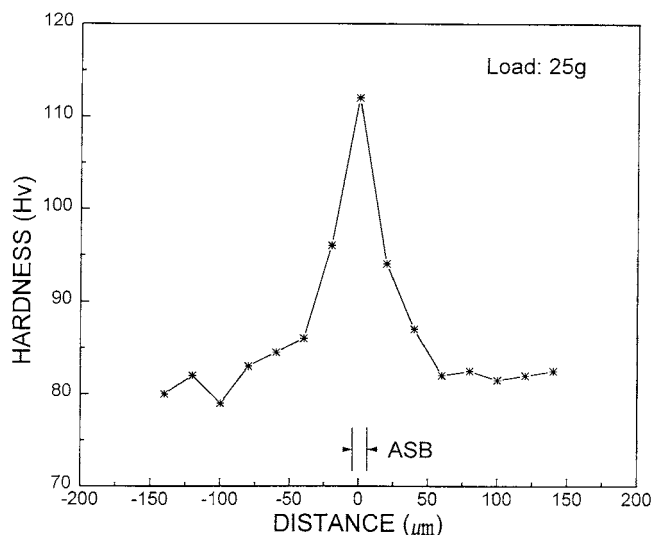


Fig. 4—Microvickers hardness data of the adiabatic shear band region.

which the grains are finer than those with a high dislocation density.

A detailed investigation of the interior of the grains within the shear band reveals a very high dislocation density, as can be seen in Figure 9(a). When the grains within the matrix far away from the shear band are examined on a specific zone axis, the existence of S' , T_1 , or θ' precipitates, as shown in Figures 5(a) through (c), can also be confirmed, since the selected area diffraction patterns associated with these precipitates can be obtained. Figures 9(b) and (c) are selected area diffraction patterns of the

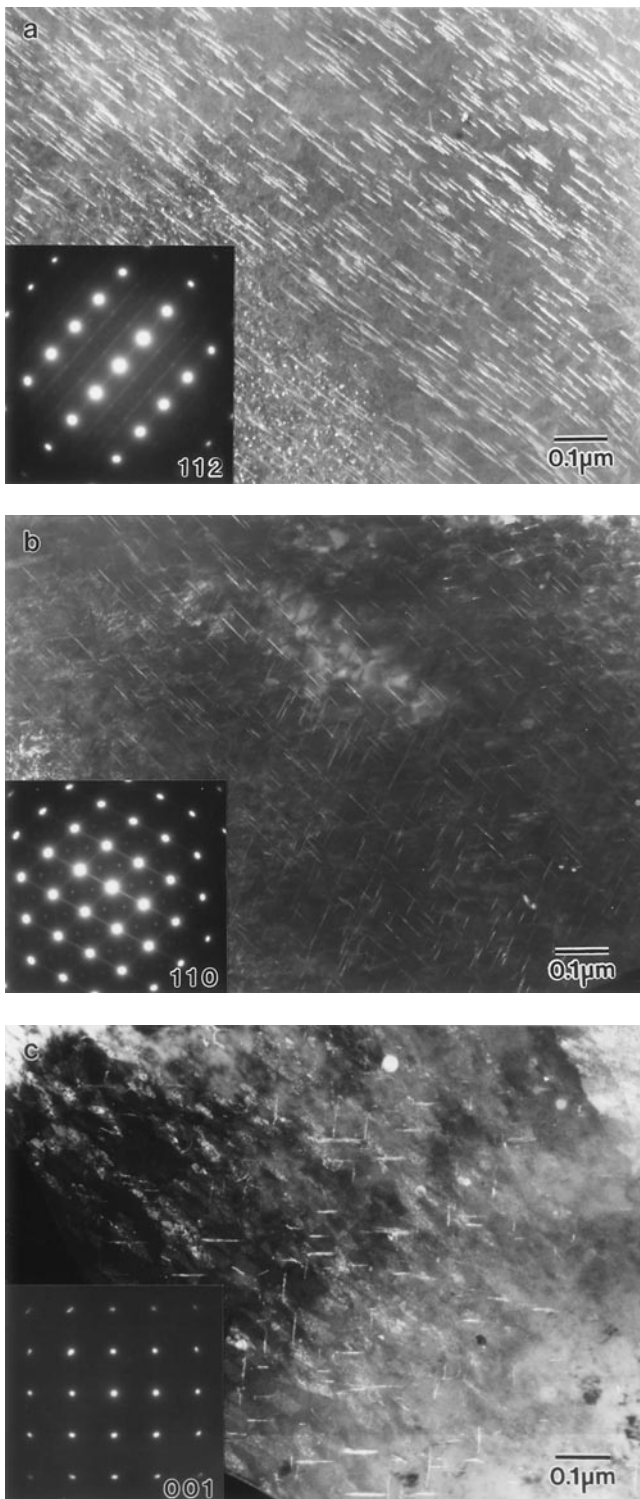


Fig. 5—Dark-field TEM images and selected area diffraction patterns of (a) S' , (b) T_1 , and (c) θ' phases, which are major precipitates of the WELDALITE alloy.

grains in Figure 9(a) at the $\langle 112 \rangle$ and the $\langle 110 \rangle$ zone axes, respectively. Comparing them with the diffraction patterns in Figures 5(a) and (b), the diffraction patterns associated with the S' and T_1 phases, which are major hardening precipitates in the WELDALITE alloy, are not observed. Neither the S' nor the T_1 or θ' phases are observed within the grains. An analysis of the grains located within the shear

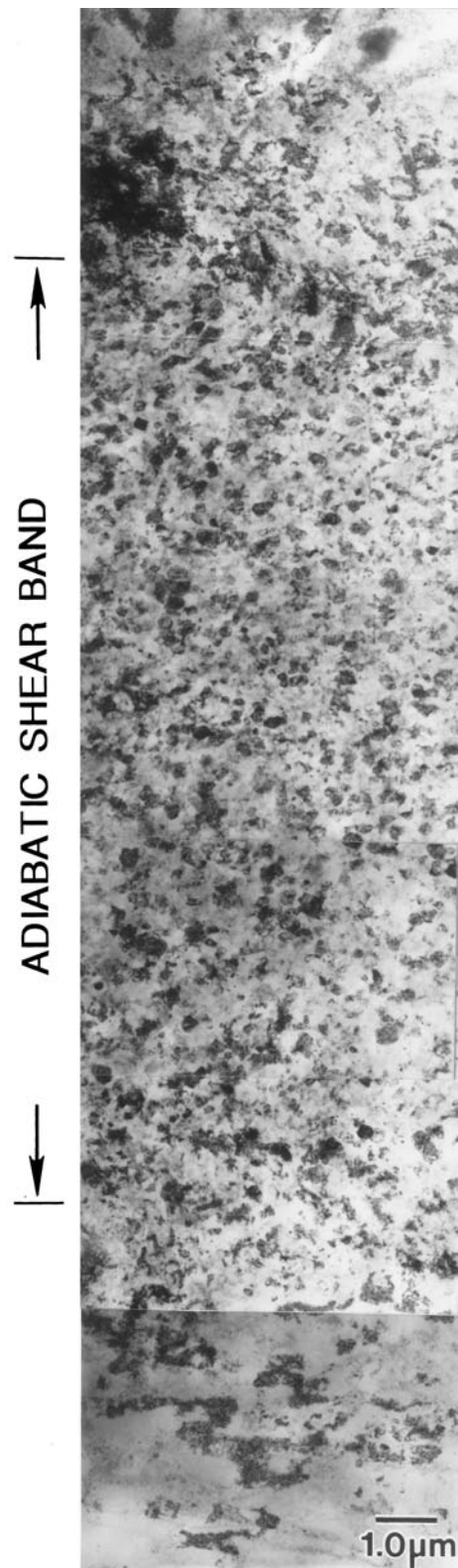


Fig. 6—Montage of bright-field TEM images spanning the entire width of the adiabatic shear band.

band by energy dispersive spectrometry shows a solid solution of Cu of about 4 to 5 wt pct. This indicates that precipitates such as S' , T_1 , and θ' existing in the original matrix are dissolved by the sudden temperature rise in the

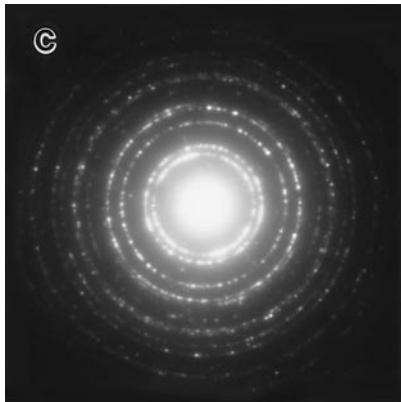
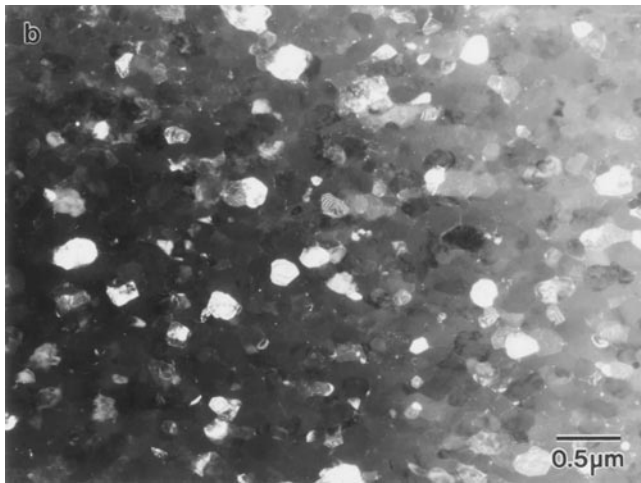
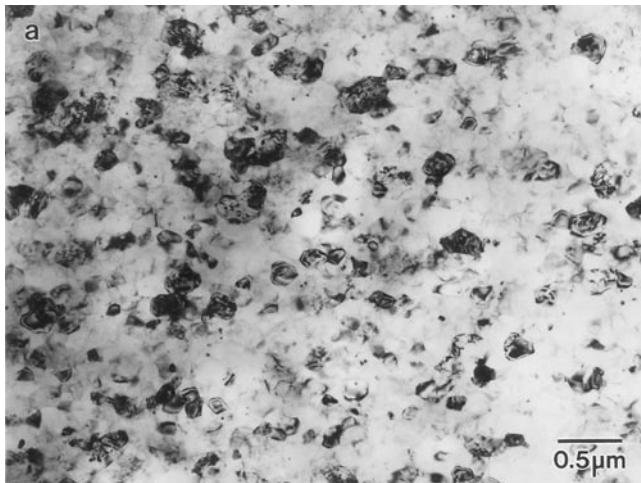


Fig. 7—TEM micrographs of the adiabatic shear band: (a) bright-field image, (b) dark-field image, and (c) selected area diffraction pattern.

process of shear band formation, resulting in a solid solution of alloying elements within the grains.

IV. DISCUSSION

The effects of temperature rise and localization of shear deformation play an important role in the microstructural development of adiabatic shear band formation. Thus, measuring the temperature rise in the dynamic deformation process provides significant data for an understanding of

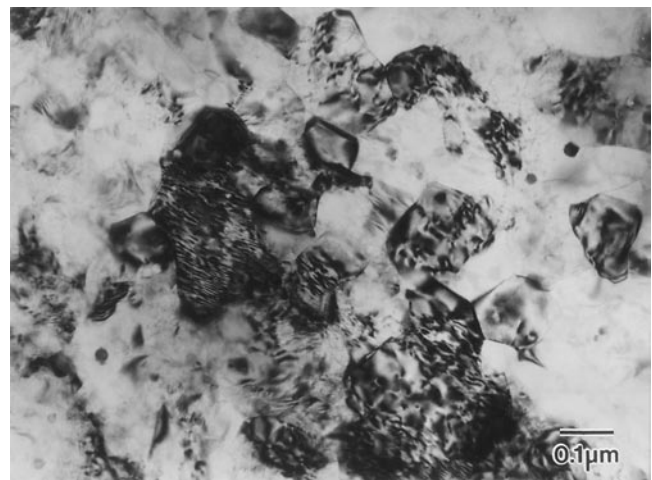


Fig. 8—TEM micrograph showing grains with very high dislocation density formed within the shear band.

the mechanism of microstructural development. Recently, Cho *et al.*^[12] measured a temperature rise of about 600 °C using an indium antimonide (InSb) detector in the dynamic torsional tests of an HY-100 steel, based on which they explained the microstructural development within the band in terms of dynamic recovery.^[13] In the present study, it was inferred by comparing the microstructures of the matrix and the band because of the inability to directly measure the temperature rise. In the WELDALITE alloy matrix, many precipitates exist, as shown in Figures 5(a) through (c), but cannot be observed in the grains within the band shown in Figures 9(a) through (c). This indicates that the precipitates are dissolved in the process of adiabatic shear band formation and that the temperature has risen above the dissolving temperature of these precipitates.

Abis *et al.*^[27] carried out a thermal analysis using differential scanning calorimetry on a 2091 Al-Li alloy, which has the same phases of T_1 , S' , and θ' as the WELDALITE alloy, and reported that the T_1 phases were dissolved at about 230 °C while the S' phases dissolved at about 270 °C. They further reported that all the precipitates within the 2091 Al-Li alloy, including the θ' phases, were completely dissolved in the range of 450 to 460 °C, irrespective of the aging conditions. The θ' phases are known to be dissolved at around 450 °C in the Al-5 pct Cu alloy.^[28] Since a large amount of copper is consumed in the precipitation process of T_1 and S' phases in the WELDALITE alloy, the dissolution temperature of the θ' phases could be lower due to the lack of copper, which can precipitate θ' phases. Although the contents of copper and lithium in the 2091 Al-Li alloy and the WELDALITE alloy are different, both have T_1 , S' , and θ' phases in common as major precipitates, but not δ' phases. Thus, it can be inferred from the observations of Figures 9(a) through (c) that the temperature has risen at least over about 460 °C in the process of shear band formation. Because 460 °C is a temperature well above 0.5 T_m (the melting point), it is high enough for dynamic recrystallization to occur within the band, considering the localization of shear deformation in a narrow area of 15 to 20 μm . In general, the dislocation density is very low within the recrystallized grains, but most of the grains recrystallized within the shear band of the WELDALITE

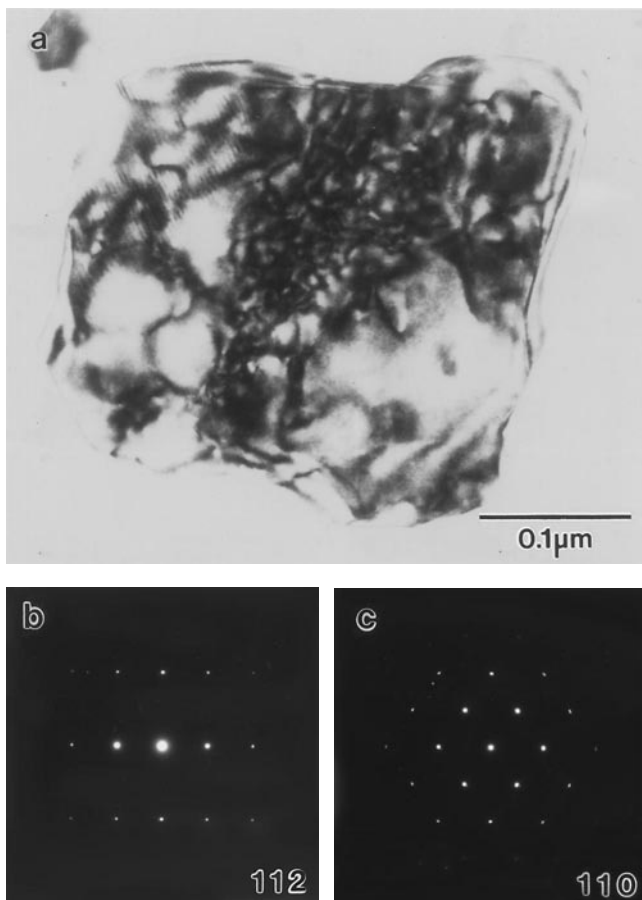


Fig. 9—(a) TEM micrograph showing a grain formed within the shear band. (b) and (c) Selected area diffraction patterns at the $\langle 112 \rangle$ and $\langle 110 \rangle$ zone axes, respectively.

alloy have a high dislocation density. This implies that continuous deformation occurred even after recrystallization in the band formation process. Due to such a continuous deformation after recrystallization and the effect of the temperature rise, the recrystallized grains can undergo another recrystallization process, resulting in finer grains. This can be inferred by the fact that grains having a lower dislocation density than the other grains and sized smaller than the average size are occasionally found and that the grains get much finer as they get nearer to the center of the shear band. This is because the most severe localized deformation and the highest temperature rise occur at the center of the band. Accordingly, it can be concluded that the deformation mechanism of the microstructural development within the adiabatic shear band of the WELDALITE alloy is a continuous dynamic recrystallization due to the localization of shear deformation and the radical temperature rise.

In fact, the temperature rise within the adiabatic shear band is related to the deformation heat generated by the plastic work. Assuming that the average shear stress and the maximum shear strain in the deformation process of the WELDALITE alloy by ballistic impact are 300 MPa and 1500 pct, respectively and that the plastic work is transformed to heat at 95 pct without any heat transfer to the nearby matrix regions, the temperature rise is calculated to be above 1000 °C at the time of the adiabatic shear band

formation. The solidus temperature of the WELDALITE alloy is reported to be above 512 °C,^[29] but the temperature could rise above it in the process of rapid temperature rising. If the temperature within the band could rise above the solidus temperature, part or all of the shear band region could be melted, depending on the degree of the rise. If melting had occurred due to the sudden temperature rise, the microstructure within the band should have shown rapidly solidified structures such as fine dendrites grown from the band/matrix boundary into the shear band by quenching from the adjacent matrix. However, in the band microstructure observed in this study, such rapidly solidified structures are not found, indicating that the temperature had not risen high enough for local melting to occur during the band formation. From these results, the temperature rise can be inferred to be above 460 °C and below the solidus temperature. However, the temperature rise cannot be measured exactly because of the inability to confirm how high the solidus temperature rises in the shear band.

The hardness of the adiabatic shear band region is much higher than that of the matrix, as shown in Figure 4. This is associated with the inter-relation of the two mechanisms of the shear band formation, *i.e.*, the hardening effect of grain refinement by the dynamic recrystallization and the high dislocation density and softening effect by the temperature rise. Because the temperature rise is the highest at the center of the shear band, it can be expected that the thermal softening effect is the highest there, but the hardening effect is also in operation due to grain refinement caused by the increased dislocation density and the dynamic recrystallization. When deformation stops, the softening effect quickly disappears because the heat is rapidly emitted into the matrix and, thus, the hardening effect predominates over the softening effect, yielding the increased hardness at the shear band. On the other hand, the microstructure in the band/matrix interfacial regions could be affected by the heat emitted from the shear band. Related to this point, Cho and coworkers^[13,21] reported on the appearance of a heat-affected zone of the HY-100 steel, in which the hardness of the zone gets lower than in the matrix due to the coarsening of carbides in the interfacial regions and the dominance of a thermal softening effect caused by dislocation recovery. However, considering the hardness variation of Figure 4, it is not likely that a heat-affected zone is formed in the WELDALITE alloy, since the heat emits rapidly due to the much-higher heat conductivity of aluminum alloys than steels.

V. CONCLUSIONS

The conclusions obtained from the present study on the microstructure of an adiabatic shear band formed by ballistic impact of a WELDALITE 049 alloy are summarized as follows

1. The microstructure of the adiabatic shear band was composed of fine recrystallized grains that had a high dislocation density. However, no precipitates could be observed in the interior of the grains.
2. It was inferred that the temperature rise in the shear band formation process was above 460 °C and below the solidus temperature. Such an inference was made from the

fact that major precipitates were dissolved and solidified structures were not found.

3. The mechanism of the microstructural development of the shear band depended on dynamic recrystallization. The feasibility of this mechanism was confirmed from the microstructural observation and the consideration of the dissolution temperature of precipitates.

ACKNOWLEDGMENTS

The authors are thankful to Professor Chang Soon Lee, Sun Moon University; Drs. Yongyun Lee and Yeung-Jo Lee, the Agency for Defence Development; and Professor Nack J. Kim, POSTECH, for their helpful discussion of the microstructural analysis.

REFERENCES

1. A.J. Bedford, A.L. Wingrove, and K.R.L. Thompson: *J. Aust. Inst. Met.*, 1974, vol. 19, pp. 61-73.
2. M.E. Backman and W. Goldsmith: *Int. J. Eng. Sci.*, 1978, vol. 16, pp. 1-99.
3. H.C. Rogers: *Ann. Rev. Mater. Sci.*, 1979, vol. 9, pp. 283-311.
4. R.J. Clifton: "Metal Response to Ultra Loading Rates," Nation Adversary Board Committee, Report No. NMAB-356, Brown University, 1980, pp. 129-42.
5. J. Wadsworth, I.G. Palmer, and D.D. Crooks: *Scripta Metall.*, 1983, vol. 17, pp. 347-52.
6. J. Wadsworth and A.R. Pelton: *Scripta Metall.*, 1984, vol. 18, pp. 387-92.
7. S.P. Timothy and I.M. Hutchings: *Acta Metall.*, 1985, vol. 33, pp. 667-76.
8. S.P. Timothy: *Acta Metall.*, 1987, vol. 35, pp. 301-06.
9. M.A. Meyers and C.L. Wittman: *Metall. Trans. A*, 1990, vol. 21A, pp. 3153-64.
10. K.A. Hartley, J. Duffy, and R.H. Hawley: *J. Mech. Phys. Solids*, 1987, vol. 35, pp. 283-301.
11. A. Marchand and J. Duffy: *J. Mech. Phys. Solids*, 1988, vol. 36, pp. 251-63.
12. K. Cho, Y.C. Chi, and J. Duffy: *Metall. Trans. A*, 1990, vol. 21A, pp. 1161-75.
13. K. Cho, S. Lee, S.R. Nutt, and J. Duffy: *Acta Metall.*, 1992, vol. 41, pp. 923-32.
14. C.L. Wittman, M.A. Meyers, and H.-R. Pak: *Metall. Trans. A*, 1990, vol. 21A, pp. 707-16.
15. A.L. Wingrove: *Metall. Trans.*, 1973, vol. 4, pp. 1829-33.
16. J.H. Beaty, L.W. Meyers, M.A. Meyers, and Nemat-Nasser: U.S. Army Materials Technical Laboratory Report No. MTL TR 90-54, United States Materials Technical Laboratory 1991.
17. M.E. Backman and S.S. Finnegan: in *Metallurgical Effects at High Strain Rates*, R.W. Rhode, B.M. Butcher, J.R. Holland, and C.H. Karnes, eds., Plenum Press, New York, NY, 1973, pp. 531-35.
18. M.A. Meyers and H.-R. Pak: *Acta Metall.*, 1986, vol. 34, pp. 2493-99.
19. M. Hartley and A.S. Martin: *Scripta Metall.*, 1984, vol. 18, pp. 449-54.
20. Y. Me-Bar and D.S. Shechtman: *Mater. Sci. Eng.*, 1983, vol. 58, pp. 181-88.
21. S. Lee, K. Cho, C.S. Lee, and W.Y. Choo: *Metall. Trans. A*, 1993, vol. 24A, pp. 2217-24.
22. K.S. Kumar, S.A. Brown, and J.R. Pickens: *Scripta Metall.*, 1990, vol. 24, pp. 1245-50.
23. W.T. Tak, F.H. Heubaum, and J.R. Pickens: *Scripta Metall.*, 1990, vol. 24, pp. 1685-90.
24. J.R. Pickens, F.H. Heubaum, and L.S. Kumar: *Scripta Metall.*, 1990, vol. 24, pp. 457-62.
25. I.J. Palmer and R.J. Chester: *Scripta Metall.*, 1989, vol. 23, pp. 1213-18.
26. B.C. Muddle and I.J. Palmer: *Acta Metall.*, 1989, vol. 37, pp. 777-89.
27. S. Abis, E. Evangelista, P. Mengucci, and G. Riontino: *Proc. 4th Int. Aluminum-Lithium Conf.*, G. Champier, B. Dubost, D. Minnay, and L. Sabety, eds., Les Editions de Physique, Paris, 1987, pp. C3-447-C3-453.
28. D.A. Porter and K.E. Esterling: *Phase Transformations in Metals and Alloys*, Van Norstrand Reinhold Co., New York, NY, 1981, pp. 291-94.
29. K.A. Montoya, F.H. Heubaum, K.S. Kumar, and J.R. Pickens: *Scripta Metall.*, 1991, vol. 25, pp. 1489-94.